Bandwidth Widening Techniques for High-Gain Antennas Based on Partially Reflecting Surfaces

Halim Boutayeb, Tayeb Denidni

BANDWIDTH WIDENING TECHNIQUES FOR HIGH-GAIN ANTENNAS BASED ON PARTIALLY REFLECTING SURFACES

Halim Boutayeb and Tayeb A. Denidni

INRS, EMT, University of Quebec, Montreal, Canada,
Email: boutayeb@emt.inrs.ca, denidni@emt.inrs.ca

ABSTRACT

In this paper, the performance in terms of frequency bandwidth of Fabry-Perot based directive antennas is first evaluated theoretically. Then, different techniques are proposed to widen the directivity bandwidth of antennas based on Partially Reflecting Surfaces. The bandwidths obtained with the proposed solutions are compared to the bandwidth obtained with a classical Fabry-Perot cavity based directive antenna.

1. INTRODUCTION

High-gain and compact antennas with of a single feed present an attractive solution for several wireless communication systems. Their single-feed system allows to increase the gain with low complexity compared to feeding networks used in conventional antenna arrays. In addition, the compactness represents an important advantage compared to parabolic antennas. To design low profile high-gain antennas with a single feed, various methods have been proposed, such as the employment of Fabry-Perot type cavities [1-4], electromagnetic crystals or zero index metamaterials [5-7].
An inconvenient of high-gain antennas based on Fabry-Perot cavities, Electromagnetic Band Gap (EBG) materials, or metamaterials is their narrow directivity bandwidth. This can represent a drawback of these antennas compared to parabolic antennas, which have a large directivity bandwidth.

In this work, we propose different techniques to widen the bandwidth of these types of antennas. Three different configurations employing Partially Reflecting Surfaces (PRSs) composed of metallic wires aree analysed. In these structures, a dipole is used for the excitation (at the center).

In Section 2, the directivity bandwidth of a simple Fabry-Perot type cavity based antenna is analysed theoretically. Then, in Section 3, a Fabry-Perot cavity with aperiodic PRSs is considered, whereas, in Section 4, a structure using two different PRSs is studied. In Section 5, the two techniques are combined. The obtained directivity bandwidth of the different configurations are compared with that of a simple Fabry-Perot based antenna.

2. EVALUATION OF THE BANDWITH OF A FABRY-PEROT CAVITY BASED DIRECTIVE ANTENNA

It is well known that the bandwidth of a Fabry-Perot based directive antenna decreases significantly when the desired gain is high. In this section, a relation between the minimum half-power beamwidth and the bandwidth is derived.
The structure shown in Fig. 1 is considered. It is composed of a Fabry-Perot type cavity composed of two Partially Reflecting Surfaces (PRS) made of metallic wires. An omni directional source is in the center of the cavity.

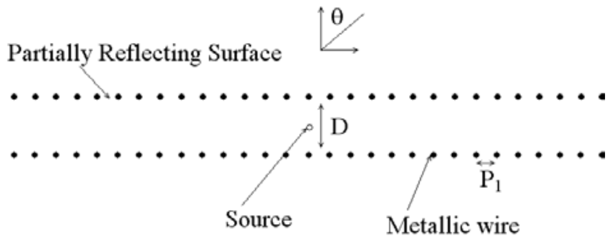

Figure 1. Principle of the Fabry-Perot cavity based directive antenna.

The frequency and angular response of the Fabry-Perot cavity to a plane wave excitation, which is in the center of the cavity, is called *T,* and it is obtained by summing all the transmitted rays [2]:

$$|T|^2 = \frac{1-|r|^2}{1+|r|^2 - 2|r|\cos(kD\cos(\theta)-\varphi_r)} \qquad (1)$$

where $r = |r|\exp(j\varphi_r)$ is the reflection coefficient of the partially reflecting surface constituted by the row of metallic wires.

For instance, we consider $|r| = 0.824$, $\varphi_r = 2.52\ rad$, and $D = 40mm$. In Fig. 2, $|T|$ is plotted versus frequency at $\theta = 0°$. The bandwidth of $|T|$ versus frequency at its half squared maximum amplitude is defined as $1/Q$, where Q is the quality factor of the cavity. Fig. 3 shows $|T|$ versus angle at different frequencies. These radiation patterns exhibit directive beams at the normal directions ($\theta = 0°$ and $\theta = 180°$) for frequencies lower than the resonant frequency f_0.

For frequencies greater than f_0, lobs appear on each side of the normal axis. $\Delta\theta_{3dB}$ is defined as the half-power beamwidth of the main lobs at the normal directions (see Fig. 3).

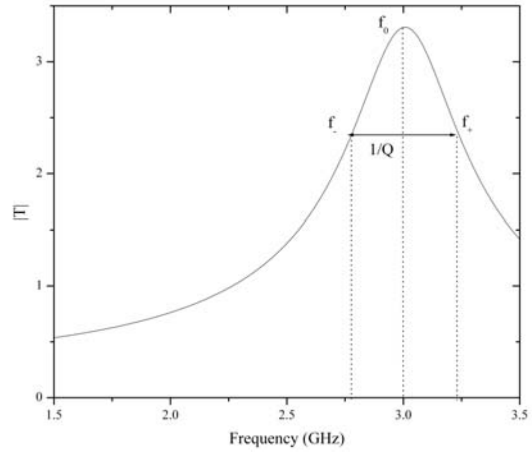

Figure 2. $|T|$ versus frequency (at $\theta = 0°$),

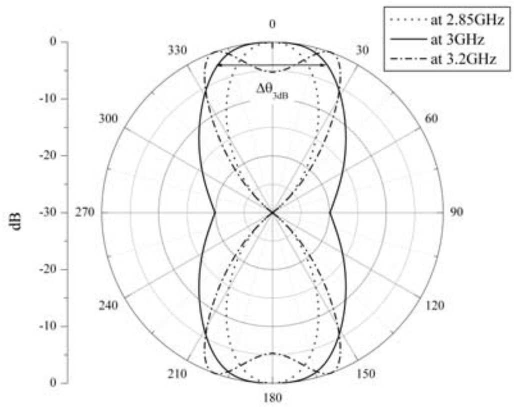

Figure 3. Normalized $|T|$ versus θ (logarithm scale) at different frequencies.

In [2], it has been shown that the half-power beamwidth can be expressed as following :

$$\Delta\theta_{3dB, f \le f_0} \approx 2\sqrt{\frac{\sqrt{2x-1}-\sqrt{x-1}}{Q}} \tag{2}$$

$$\Delta\theta_{3dB, f_0 \le f \le f^+} \approx 2\sqrt{\frac{\sqrt{x-1}+1}{Q}} \tag{3}$$

where $x = |T|^2_{\max} / |T|^2$.

The minimum half-power beamwidth is obtained for f<f$_0$ (Eq. (2)) and for x = 1.5:

$$\Delta\theta_{3dB\min} \approx \sqrt{\frac{4}{\sqrt{2Q}}} \tag{4}$$

Note that Eq. (4) is a little different from the formula in [2], where there is a minor error.

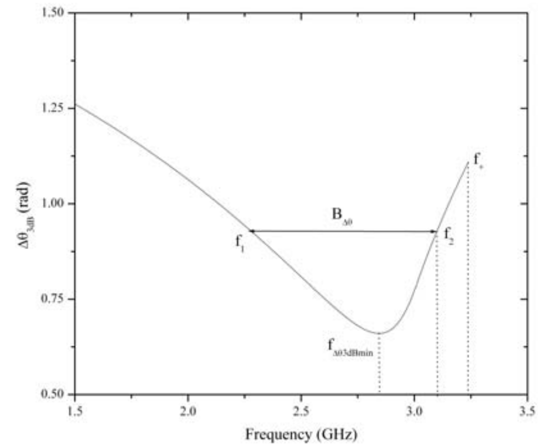

Figure 4. $\Delta\theta_{3dB}$ (Eqs. (2) and (3)).

By using Eqs. (2) and (3), the half-power beamwidth $\Delta\theta_{3dB}$ is plotted in Fig. 4 as a function of the frequency, for the considered example.

In Fig. 4, f_1 and f_2 are the frequencies for which $\Delta\theta_{3dB} = \sqrt{2}\Delta\theta_{3dB,\min} = 2\sqrt{\frac{\sqrt{2}}{Q}}$. The coefficients x_1 and x_2, corresponding to f_1 and f_2, respectively, were calculated numerically from Eqs. (2) and (3): $x_1 \approx 10.985$, $x_2 \approx 1.175$.

From this, and using the relation $\frac{1}{Q_x} \approx \sqrt{x-1}\frac{1}{Q}$ [2], we obtain :

$$2\frac{f_0 - f_1}{f_0} = \frac{1}{Q_{x1}} \approx \frac{\sqrt{9.895}}{Q} \tag{5}$$

then

$$f_1 \approx f_0\left(1 - \frac{\sqrt{9.895}}{2Q}\right) \tag{6}$$

We have also

$$2\frac{f_2 - f_0}{f_0} = \frac{1}{Q_{x2}} \approx \frac{\sqrt{0.175}}{Q} \tag{7}$$

and then

$$f_2 \approx f_0\left(1 - \frac{\sqrt{0.175}}{2Q}\right) \tag{8}$$

Now, one can calculate the bandwidth between f_2 and f_1:

$$B_{\Delta\theta} = 2\frac{f_2 - f_1}{f_2 + f_1} = 2\frac{\sqrt{9.895}+\sqrt{0.175}}{4Q - \sqrt{9.895}+\sqrt{0.175}} \tag{9}$$

By using Eq. (4), the following relation is obtained:

$$B_{\Delta\theta} = 2\frac{\left(\sqrt{0.175}+\sqrt{9.895}\right)\left(\frac{\Delta\theta_{3dB\min}}{2}\right)^2}{2\sqrt{2}+\left(\sqrt{0.175}-\sqrt{9.895}\right)\left(\frac{\Delta\theta_{3dB\min}}{2}\right)^2} \quad (10)$$

$B_{\Delta\theta}$ is the frequency bandwidth where the half-power beamwidth is less than $\sqrt{2}$ times the minimum half-power beamwidth.

Using Eq. (10), the bandwidth $B_{\Delta\theta}$ is plotted versus the minimum half-power beamwidth in Fig. 5. This curve characterizes the performance of Fabry-Perot cavity based directive antennas. It can be seen that the beamwidth decreases drastically when the minimum half-power beamwidth is small.

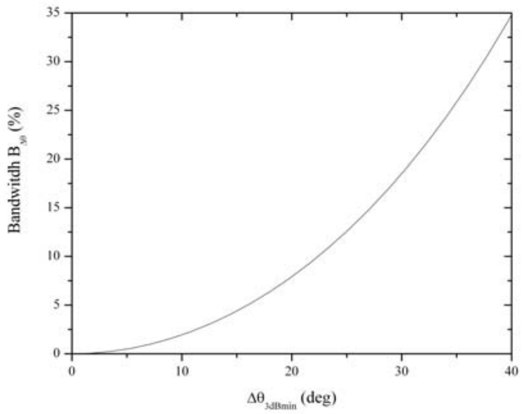

Figure 5. $B_{\Delta\theta}$ vs. $\Delta\theta_{3dB\min}$ (Eq. (10))

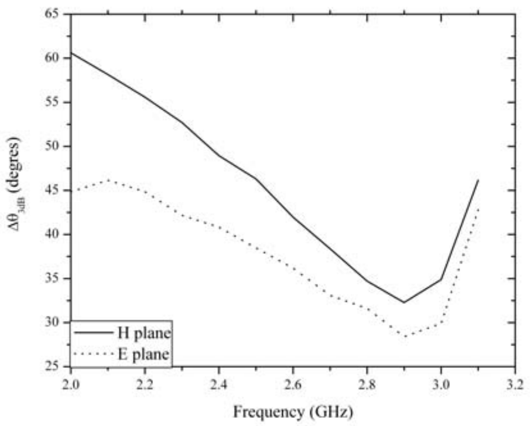

Figure 5. $\Delta\theta_{3dB}$.

For instance, we consider that the wires are $56cm$ length and $2\ mm$ diameter, the number of wires in each row is 28, the cavity is $D = 40\ mm$ width, the period is $P = 20\ mm$, and the dipole is $65\ mm$ length and $2\ mm$ diameter. The structure was simulated with a Finite Difference Time Domain (FDTD) code. For the considered example, the half-power beamwidth in H-plane, and E-plane, is plotted vs. frequency in Fig. 6. From this figure, the bandwidths $B_{\Delta\theta}$ are 20% and 23.8%, in the H-plane and E-plane respectively. These results agree with the results predicted by Eq. (10) and illustrated in Fig. 5.

Now, it is of interest to find a structure which presents the same minimum beamwidth but with larger bandwidth. It is clear that antennas based on electromagnetic crystals or zero index metamaterials [5-7] are not good candidates. In the next sections we investigate two techniques to widen the bandwidth of a directive antenna based on Partially Reflecting Surfaces.

3. USING AN APERIODIC PRS

A first method in order to increase the directivity bandwidth of the antenna consists on using a non-uniform PRS. If one use a PRS which presents a phase of the reflection coefficient increasing with incidence angle, the bandwidth will increase. Indeed, the resonant frequency at the angle θ, can be written [2] :

$$f_{0,\theta} = \frac{c\varphi_r(\theta)}{2\pi D\cos(\theta)} \quad (11)$$

where c is the speed of light and φ_r is the phase of the reflection coefficient r. From Eq. (11), if φ_r increases significantly with the angle θ, the resonant frequencies for angle higher than 0° will be shifted to higher frequencies, and the frequency f^+ (see Fig. 4) will be shifted to higher frequency.

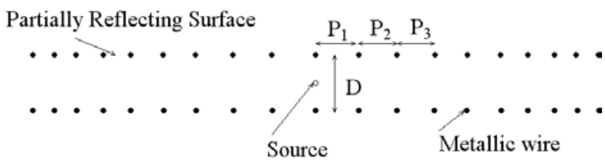

Figure 6. Directive antenna based on an aperiodic PRS.

P_1	20 mm
P_2	20 mm
P_3	17.5 mm
P_4	17.5 mm
P_5	17.5 mm
P_6	17.5 mm
P_7	15 mm
P_8	15 mm
P_9	15 mm
P_{10}	15 mm
P_{11}	12.5 mm
P_{12}	12.5 mm
P_{13}	12.5 mm
P_{14}	12.5 mm
P_{15}	10 mm
P_{16}	10 mm
P_{17}	10 mm
P_{18}	10 mm

Table 1. Spacing between wires in the aperiodic PRS

We propose to change the period of the PRS, as illustrated in Fig. 6, in order to obtain a coefficient φ_r increasing with incidence angle.

The example with the specifications indicated in Tab. 1, is considered. The dimensions of the antenna (length, larger and dipole dimensions) are the same than previously.

In Figs. 7 and 8, the half-power beamwidths are plotted in the H-plane and the E-plane respectively, for the structure with aperiodic PRSs and for the structure with periodic PRS. From these figures, one can see that the aperiodic PRS allows to decrease the half-power beamwidth after the resonant frequency (f_0=3GHz). In the E-plane (Fig. 8), a widening of the bandwidth is also observed.

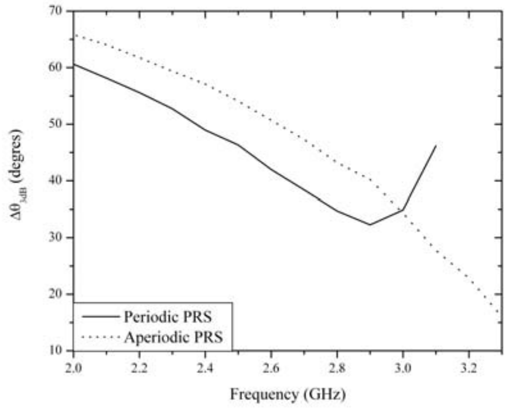

Figure 7. $\Delta\theta_{3dB}$, H-plane

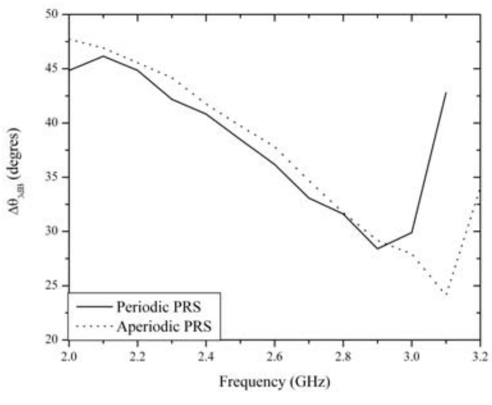

Figure 8. $\Delta\theta_{3dB}$, *E-plane*

4. USING TWO DIFFERENT PRSs

Another method for increasing the directivity bandwidth consists on using two different PRSs, as illustrated in Fig. 9. The use of multiple cavities allows to modify the response of the structure (*ie*. *T*), and then the curve of the half-power beamwidth. In Fig. 9, the PRSs are spaced by the distance D=35mm, and the two periods are P_1=20mm, P_2=40mm. Figs. 10 and 11 present the simulated half-power beamwidth of the antenna in the H-plane and E-plane.

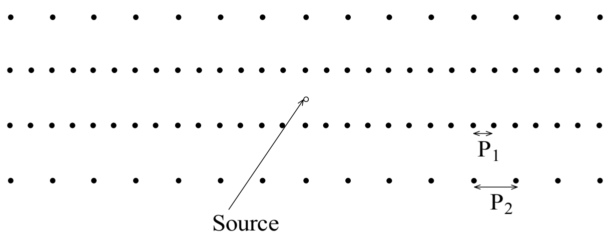

Figure 9. Directive antenna based on two different PRSs

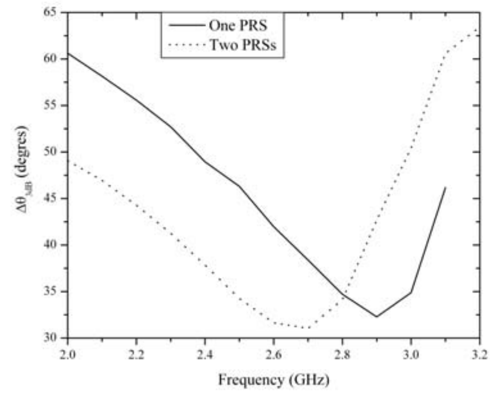

Figure 10. $\Delta\theta_{3dB}$, *H-plane*

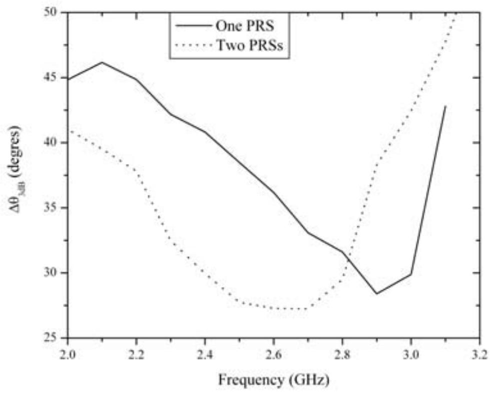

Figure 11. $\Delta\theta_{3dB}$, *E-plane*

From Figs. 10 and 11, the bandwidths are 27%, in both H-plane and E-plane. The two structures, the structure with two different PRSs and the structure with one PRS, have the same minimum half-power beamwidth, but the structure with two different PRSs has a larger bandwidth. From this, the structure using two different PRSs has a better performance.

5. COMBINATION OF THE TWO TECHNIQUES

A structure combining the two previous techniques, shown in Fig. 12, is now considered. The dimensions of the antenna are to the previous ones ($56 \times 56 cm^2$, D=35mm). Figs. 13 and 14, present the half-power beamwidth in the H-plane and the E-plane.

From Figs 1 and 14, with the proposed structure, the bandwidths are 32% and 34%, in the H-plane and E-plane, respectively, which represent a widening of 60% and 42% by comparison with the bandwidths obtained with the simple Fabry-Perot cavity structure.

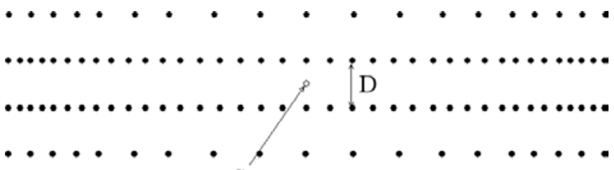

Figure 12. Directive antenna based on two aperiodic PRSs.

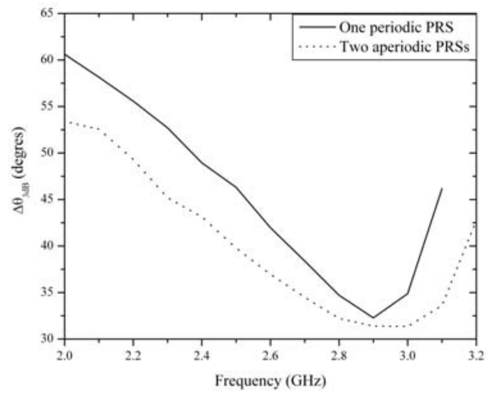

Figure 13. $\Delta\theta_{3dB}$, H-plane.

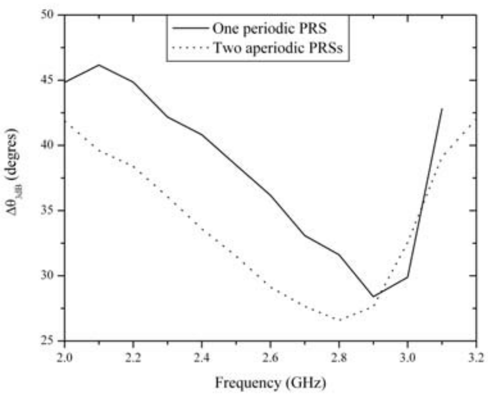

Figure 14. $\Delta\theta_{3dB}$, E-plane.

6. CONCLUSION

A theoretical analysis of the bandwidth of directive antennas based on a Fabry-Perot cavity composed of two Partially Reflecting Surfaces has been presented. To widen the bandwidth of these types of antennas, two techniques have been proposed. The first technique consists on varying the distance between elements in the Partially Reflecting Surface. The second technique consists on using different PRSs. A third configuration combining the two techniques has also been analysed in order to obtain a larger bandwidth. Numerical results obtained with a full wave method have been presented, showing the usefulness of the proposed approach.

Structures with more Partially Reflecting Surfaces and using other variations in the distance between elements of the PRSs can be analysed to increase more the bandwidth of these type of antennas.

REFERENCES

[1] T. Akalin, J. Danglot, O. Vanbesien, and D. Lippens, “A highly directive dipole antenna embedded in a Fabry-Perot type cavity”, IEEE Microwave Wireless Comp. Lett., vol. 12, pp. 48-50, Feb. 2002.

[2] H. Boutayeb, K. Mahdjoubi, A.C. Tarot, and T. Denidni, “Directivity of an antenna embedded inside a Fabry-Perot cavity : Analysis and Design”, Microw. Opt. Technol. Lett., vol. 48, pp. 12-17, Jan. 2006.

[3] N. Guerin S. Enoch, G. Tayeb, P. Sabouroux, P. Vincent, H. Legay, “A metallic Fabry-Perot directive antenna”, IEEE Trans. On Anten. And Propag. 54 (2006), pp. 220-224

[4] A.P. Feresidis, G. Goussetis, S. Wang and J.C. Vardaxoglou, “Artificial magnetic conductor surfaces and their application to low-profile high-gain planar antennas” IEEE Trans. Antennas Propag., vol. 53, pp. 209-215, Jan. 2005.

[5] C. Cheype, C. Serier, M. Thevenot, T. Monediere, A. Reineix and B. Jecko, “An Electromagnetic Bandgap resonator antenna” IEEE Trans. Antennas Propagat., vol. 50, pp. 1285-1290, Sept. 2002.

[6] S. Enoch, G. Tayeb, P. Sabouroux, N. Guerin, and P. Vincent, “A metamaterial for directive emission” Phys. Rev. Lett., vol. 89, no. 21, pp. 213902-1-213902-4, Nov. 2002.

[7] H. Boutayeb and T.A. Denidni, “Analysis and Design of a High-Gain Antenna based on Metallic Crystals”, Journal of Electromagnetic Wave and Application, Vol. 20, No. 5, 599–614, 2006.